Applied Surface Science 385 (2016) 562–568

Contents lists available at ScienceDirect

Applied Surface Science

journal homepage: www.elsevier.com/locate/apsusc

A simple approach to fabricate the rose petal-like hierarchical surfaces for droplet transportation

Chao Yuan, Mengyu Huang, Xingjian Yu, Yupu Ma, Xiaobing Luo*

State Key Laboratory of Coal Combustion, School of Energy and Power Engineering, Huazhong University of Science and Technology, Wuhan 430074, China

ARTICLE INFO

Article history:
Received 13 April 2016
Received in revised form 16 May 2016
Accepted 23 May 2016
Available online 25 May 2016

Keywords:
Electroless galvanic deposition
Sticky superhydrophobic surfaces
Fabrication
Copper substrate
Droplet transportation

ABSTRACT

Precise transportation of liquid microdroplets is a great challenge in the microfluidic field. A sticky superhydrophobic surface with a high static contact angle (CA) and a large contact angle hysteresis (CAH) is recognized as the favorable tool to deal with the challenging job. Some approaches have been proposed to fabricate such surface, such as mimicing the dual-scale hierarchical structure of a natural material, like rose petal. However, the available approaches normally require multiple processing steps or are carried out with great expense. In this study, we report a straightforward and inexpensive method for fabricating the sticky superhydrophobic surfaces. The fabrication relies on electroless galvanic deposition to coat the copper substrates with a textured layer of silver. The whole fabrication process is carried out under ambient conditions by using conventional laboratory materials and equipments, and generally take less than 15 min. Despite the simplicity of this fabrication method, the rose petal-like hierarchical structures and the corresponding sticky superhydrophobic wetting properties were well achieved on the artificial surfaces. For instance, the surface with a deposition time of 10 s exhibits the superhydrophobity with a CA of 151.5°, and the effective stickiness with a CAH of 56.5°. The prepared sticky superhydrophobic surfaces are finally shown in the application of droplet transportation, in which the surface acts as a mechanical hand to grasp and transport the water droplet.

1. Introduction

In the past decade, numerous studies [1–4] have focused on the design of "slippery" superhydrophobic surfaces by mimicking the dual-scale hierarchical structure of lotus leaves on which the microscopic epidermal cells (3–11 μm diameter and 7–13 μm height) are decorated with the nanoscopic wax crystals (100 nm) [5]. These surfaces have a high static contact angle (CA) (>150°) and a low contact angle hysteresis (CAH) (<10°). The low CAH implies that the surface has low adhesion and friction to water. Consequently, the water droplets on such surfaces cannot remain stable, but spontaneously roll off. Due to the distinct wettability, the slippery superhydrophobic surfaces have been used in various commercial and industrial fields, including paints, textiles, water repellence, dirt-removal, oil-water separation and low-friction surfaces for fluid flow and energy conservation [6–9]. On the other hand, in the microfluidic field, the researchers usually have the difficultly in conducting the analysis on very small volumes of liquid samples and transporting the liquid microdroplets over a surface without any loss or contamination. In such circumstances, a "sticky" superhydrophobic surface with large CAH (or adhesion) is recognized as the favorable tool to meet the researchers needs [10]. Such surface has the special properties that the water droplet, which remains spherical in shape (CA > 150°), stays pinned to the surface and does not roll off even if the surface is turned upside down. Therefore, in the application of droplet transportation, the sticky superhydrophobic surface can act as a"mechanical hand" to grasp and transport the droplet [10].

Although the sticky superhydrophobic surface has significant applications, few attentions have been paid on its fabrication comparing with slippery superhydrophobic surface. It is reported [11] that rose petal is such a surface having a large CAH, as well as high CA. It also shows the micro- and nanoscale hierarchical structure. However, its microstructures, formed by micropapillaes (16 μm diameter and 7 μm height) [11], have a larger pitch value than the lotus leaf [12]. Inspired from the structures of rose petal, the sticky superhydrophobic surfaces were achieved artificially with several approaches, including photolithography followed by thermal evaporation [12], photolithography followed by spin-coating [13] and fluorination of raspberry-like particles [14]. These approaches yield the surfaces exhibiting superhydrophobicity with large CAH, but require multiple processing steps. The rose petal-like surfaces have also been obtained by one-step direct methods, such as femtosecond laser [15], dielectric barrier discharge [16] and electrospinning

* Corresponding author.
E-mail address: luoxb@hust.edu.cn (X. Luo).

http://dx.doi.org/10.1016/j.apsusc.2016.05.128
0169-4332/

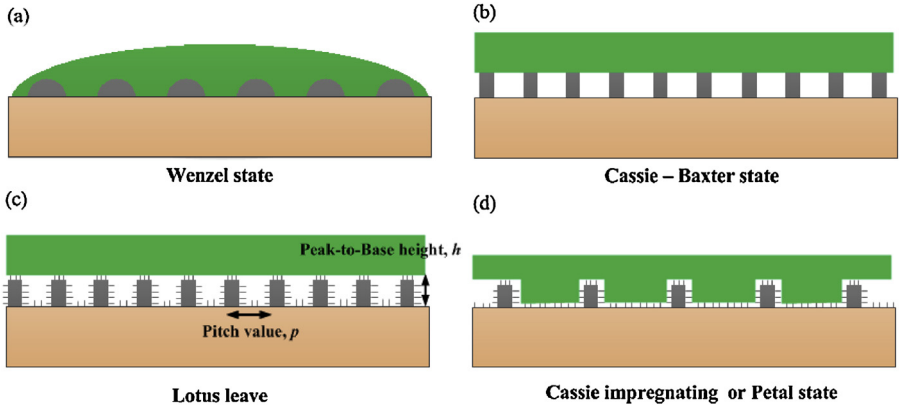

Fig. 1. Schematic of wetting scenarios. (a) Wenzel state, (b) Cassie state, (c) Lotus leaf and (d) Petal state.

[17]. However, applying these approaches is still not cost-effective in many applications.

Electroless galvanic deposition is considered to be a remarkably straightforward and cost-effective approach to fabricating superhydrophobic surfaces [18]. This approach coats a metal substrate with a textured layer of a second metal by galvanic deposition. Subsequent immersion of the coated sample in a surface modifier covers the textured layer with a low surface free energy monolayer and renders it hydrophobic. The deposition of the coating metal naturally generates the double roughness structures which are made up of 0.2–1 μm clusters constructed from smaller agglomerated primary particles (50–200 nm). In the study [18], since the deposition time is long enough, the microscale clusters is observed to be compact and like lotus leaf more than rose petal. Accordingly, the prepared sample displays the great slippery superhydrophobic property with CA more than 170° and roll-off angle less than 1° [18]. Due to these advantages, the approach has been applied to fabricate the low-friction surfaces in various applications [19–21]. However, most of these works only focused on the realization of superhydrophobic surfaces. Little is known about the influence of different dual-scale structures on the surface wettability. In addition, none of works has been carried out for the fabrication of sticky superhydrophobic surfaces with this approach.

In this study, we present a remarkably straightforward method for fabricating the sticky superhydrophobic surfaces. The fabrication relies on electroless galvanic deposition to form the pre-defined structured on metal surfaces, which yield robust sticky superhydrophobic property. The whole fabrication process is under ambient conditions using conventional laboratory materials and equipment, and generally take less than 15 min. The outline of this study is as follows. At first, we introduce the wetting mechanisms of the water droplets on rough solid surfaces. On the basis of the mechanisms, a synthetic procedure that enables the rose petal-like hierarchical structure on artificial surfaces is then described. After that, the morphologies of the surfaces are observed on micro- and nanometer scales to prove the formation of distinct structures on artificial surfaces. Subsequently, the sticky superhydrophobic property of the samples is verified by measuring the static CA and CAH. Finally, the application of the sticky superhydrophobic surface is demonstrated by a droplet transportation process.

2. Backgrounds

There are two models or states to describe the wettability of rough surfaces: the homogeneous (Wenzel) [22] and the composite (Cassie-Baxter) [23] models. As schematically illustrated in Fig. 1a, the Wenzel state describes that the liquid completely fills the valleys of a rough solid surface. Cassie-Baxter extended Wenzel's model for a heterogeneous surface composed of two different materials. As shown in Fig. 1b, the model describes that a gaseous phase, normally referred to as "air", may be trapped in the valleys of the structure, resulting in a composite solid-liquid-air interface. The Cassie-Baxter model indicates that increasing the roughness may result in the formation of air pockets, leading to the increase of CA and the decrease of CAH [24].

It is well known [16,25,26] that for the lotus leaf (schematically illustrated in Fig. 1c), the small pitch value (p) and the large peak-to-base height (h) make the droplets on this surface to be Cassie-Baxter state. In contrast, the rose petal's microstructure (schematically shown in Fig. 1d) has a larger p and a smaller h [12,16,17,27]. Thus, the liquid is allowed to impregnate between the microstructure. This is referred to as the Cassie impregnating wetting state or petal state, in which the wetted surface area is greater than that in the Cassie-Baxter state but less than that in the Wenzel state [12]. In this state, both CA and CAH values can be large, resulting a remarkable adhesive force for the water droplet sticking to the surface.

From the understanding of wetting mechanisms, the artificial sticky superhydrophobic surface can be obtained by controlling the dual-scale structure to have a large p and small h. As described above, the former investigation [18] has applied the electroless galvanic deposition method to fabricate the slippery superhydrophobic surfaces. With the long deposition time, the microstructure shows a much smaller p. Therefore, it is possible to fabricate the sticky superhydrophobic surface by shortening the deposition time to enlarge p of microstructure.

3. Experimental

3.1. Surfaces preparation

The superhydrophobic surfaces with high CAH were prepared on copper plates with dimensions of 30 × 30 mm. The plates were mechanically polished to mirror finish before preparation. The reagents used in the fabrication were listed as follow: AgNO3 (99%), 1H, 1H, 2H, 2H-perfluorodecanethiol (HDFT, 97%, Aldrich), 1, 2-dichloromethane (DCM, 99%), acetone and deionized water.

Fig. 2 schematically shows the simple and facile way of preparing sticky superhydrophobic surfaces. These surface are prepared with short deposition time (t). For the purpose of comparison, slippery superhydrophobic surfaces were also fabricated with long t. Firstly, the polished plates were cleaned with acetone. Subsequently, several pieces of plates were put into a container synchronously which held 50 mL aqueous $AgNO_3$ solution (0.010 mol dm^{-3}) with a temperature of 25 °C. A silver structure was produced at the plate surface by electroless galvanic deposition. t for each plate was controlled precisely: after a given time

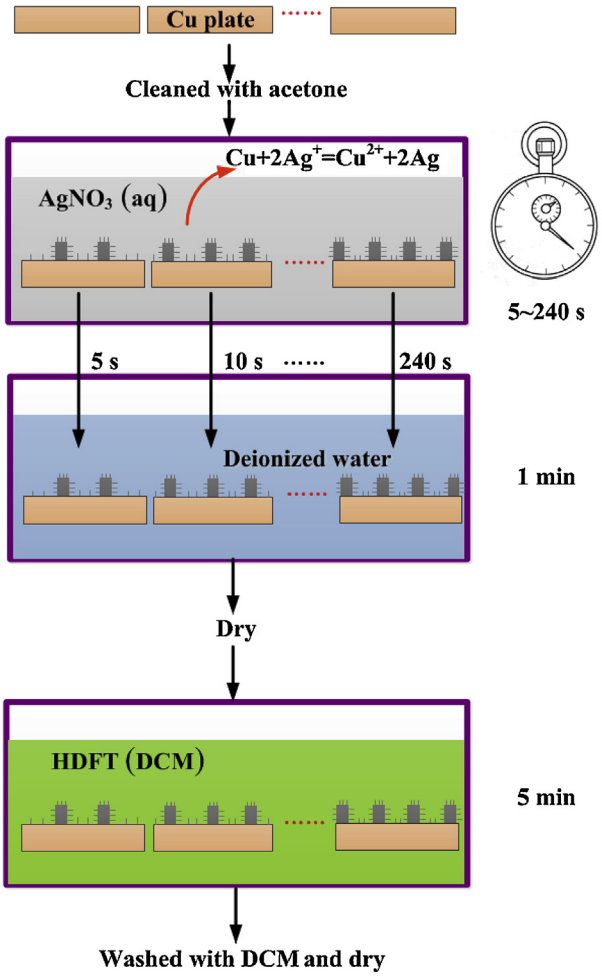

Fig. 2. Schematic illustration of surfaces fabrication.

period (5–240 s), the plates were taken out and immersed into 100 mL deionized water in sequence. After 1 min, all plates were removed and dried with compressed air. Then, all plates were immersed into a HDFT solution in DCM (0.001 mol dm^{-3}) for 5 min. Finally, the plates were washed twice with fresh DCM and dried under normal atmosphere. The entire process was performed under ambient conditions at 25 °C and carried out on two groups of copper plates.

3.2. Surface characterization

The morphologies of the silver-coated surfaces were observed on micro- and nanometer scales using scanning electron microscope (SEM) and atomic force microscope (AFM). SEM and AFM were carried out with FEI Sirion-200 and Shimadzu SPM-9700, respectively. The AFM image covers an area of 5 × 5 μm.

Static CA and CAH were measured using an optical contact angle meter (Kruss, DSA25). For the measurement of static CA, the droplet size should be smaller than the capillary length, but larger than the dimension of the microstructures on the surfaces [28]. In this study, 4.5 μL of deionized water droplets (with diameter of about 2 mm) was gently deposited on the surfaces using a microsyringe. A picture of the droplet was taken after a few seconds to avoid any problems related to the droplet. Tangent measurement was made on the profile of the droplet to obtain the value of CA. For each sample, three images (six angles) were taken to get the average value. CAH is defined as the difference between the advancing contact angle and receding contact angle. The advancing and receding angle measurements were made using the dynamic sessile drop method [16,25]: perform the CA measurements starting with a 3 μL droplet which was slowly increased to 10 μL and decreased to 3 μL at 0.5 μL increment step. Advancing angle is the possible maximum contact angle for the drop without the contact line moving when adding volume, while receding angle corresponds to the possible minimum contact angle upon removing volume.

3.3. Droplet transportation

Droplet transportation was conducted to present the application of sticky superhydrophobic surfaces. Two processes were recorded with a high-speed camera (Photron, SA3). The first process is to use a prepared sticky superhydrophobic surface to grasp a small water droplet from a slippery superhydrophobic surface. The second is to transfer the droplets to a hydrophilic surface. Since the length of shooting time is limited for the high-speed camera, two processes were recorded separately.

4. Results and discussion

4.1. Characterization of surface structure

Fig. 3 provides the SEM images of the surfaces with t from 10 s to 40 s. The low-magnification micrographs shows that the silvers are deposited line-by-line on the copper plates. The formation of parallel structures is related to the nucleation of silvers, which incline to nucleate along the parallel scratches left by mechanically polishing the copper substrates. It is observed from the medium- and high-magnification images that the coating metals naturally generates hierarchical structures on surfaces, which are made of microscale clusters (0.8–3 μm) constructed from smaller agglomerated nanoparticles (50–800 nm). Fig. 4 also shows the 3D AFM topography images. These images for microstructure and nanostructure illustrates the similar morphology to that in the SEM micrographs.

Although the dual-scale structure is observed easily on all surfaces, the microstructures of them show a great disparity. Firstly, when the deposition time is ranging from 10 s to 20 s, apart from the clusters, there exist some independent micro- or nanoparticles (indicated by red arrows in the SEM images), which have not yet constructed the dual-scale structure. While, after 20 s, almost all particles are found to form the hierarchical structures based on the observation of high-magnification SEM images of Fig. 3c–d. In addition, comparing the medium-magnification SEM images, the microstructures are shown to be more compact with t increasing. The average dimensions of clusters are also found to increase with t when comparing the high-magnification SEM and AFM images. Using the SEM and AFM images, the statistical parameters of microstructure, including p, clusters diameter (d) and h, are obtained and summarized in Table 1. In this work, p is estimated using another statistical parameter, clusters density (f), which is defined as the average number of clusters counted in the medium-micrographs with an area of 22.5 × 17.5 μm^2. The lower f implies the larger values of p. d is measured using high-magnification SEM images and h is assumed to be the maximum height of roughness profile derived from the AFM images. From the data, we can find that the surfaces with shorter t (10–20 s) have the larger p and smaller d and h.

In addition to microstructures, there is a slight disparity of nanostructures among the surfaces. Through observing the high-magnification SEM images, the geometry of the nanoparticles, composing the microscale clusters, are identified and summarized in Table 1. When t is 10 s, the nanoparticles exhibit a platelet shape. As t increases, the nano-platelets become nano-spheres with a larger surface area.

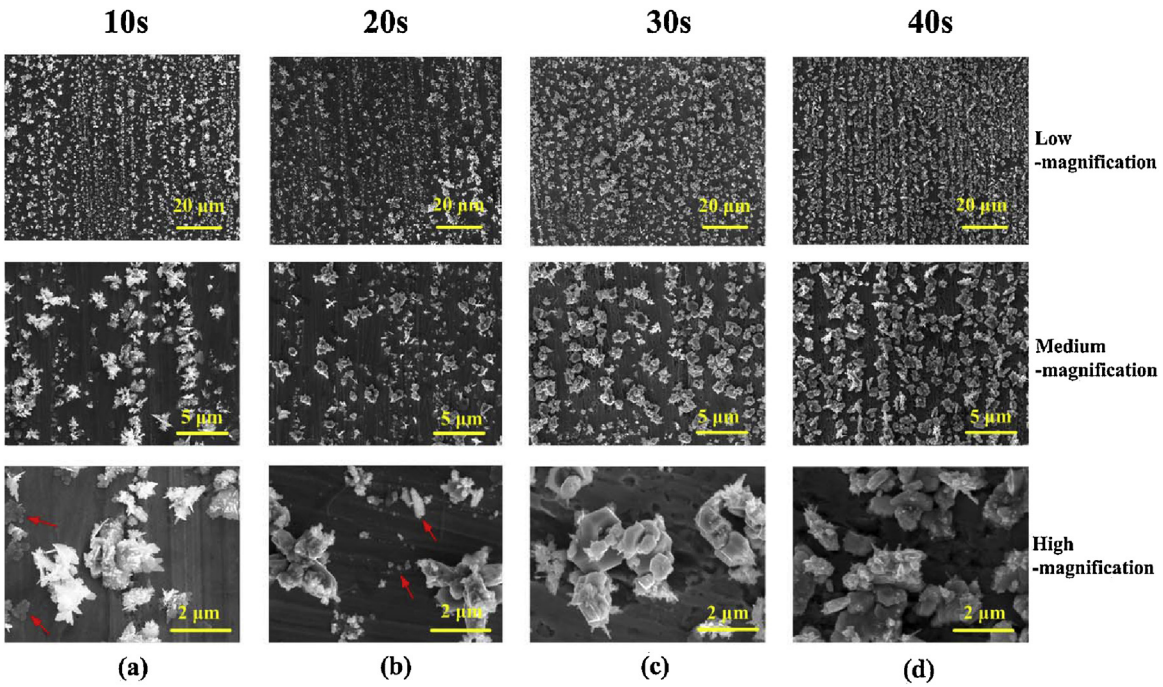

Fig. 3. SEM images of silver-deposited copper surfaces with different deposition time: (a) 10 s, (b) 20 s, (c) 30 s and (d) 40 s. (For interpretation of the references to color in the text, the reader is referred to the web version of this article.)

4.2. Characterization of surface wettability

As expected, the sticky superhydrophobic property is achieved on the surfaces fabricated with relative short *t*. One of the examples is shown in Fig. 5, which was prepared with 20 s. The high CA (155.1°) presented by Fig. 5a proves the achievement of superhydrophobicity on that surface. Furthermore, tilting experiments present its sticky property. As shown in Fig. 5b–c, despite high CA, small water droplets (3.5 μL) can stick to the surface and does not roll off when the surface was tilted at 80° (Fig. 5b) or turned upside down (Fig. 5c).

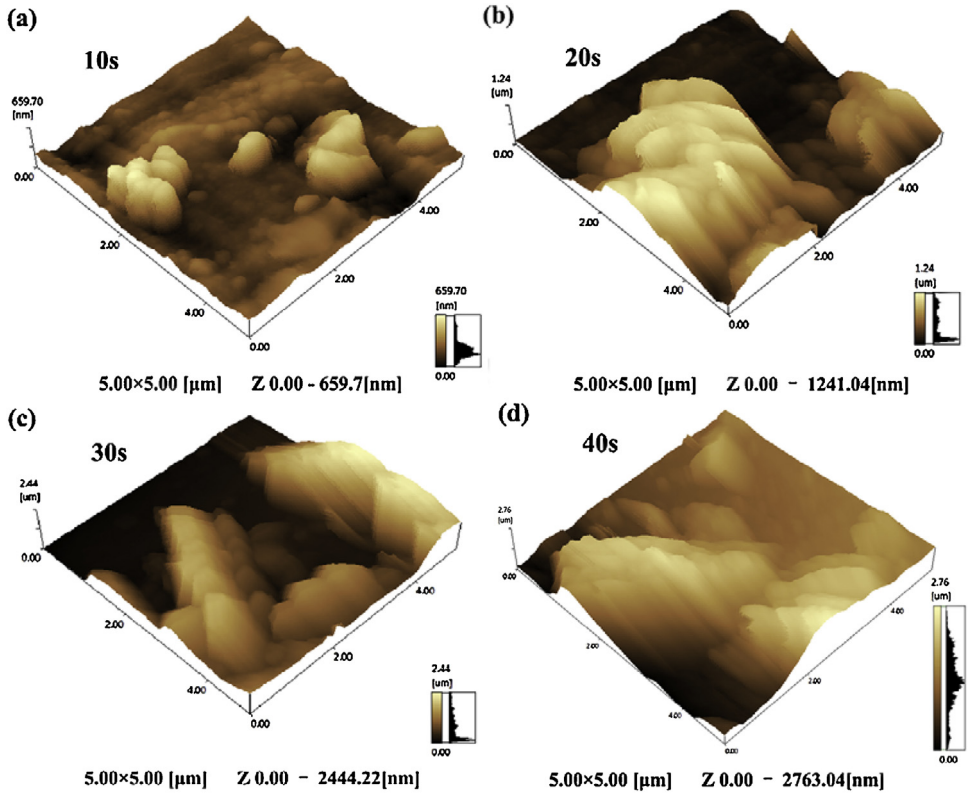

Fig. 4. AFM images of silver-deposited copper surfaces with different deposition time: (a) 10 s, (b) 20 s, (c) 30 s and (d) 40 s.

Table 1
Summary of morphology, microstructure statistics and nanostructure geometry for the silver-deposited surfaces with different deposition time.

Deposition time (s)	Morphology	Clusters density (1/394 μm²)	Clusters diameter (μm)	peak-to-base height (μm)	Nanostructure geometry
10	Clusters and independent particles	70	1–2.4	0.66	Platelet
20	Clusters and independent particles	74	0.8–2.6	1.24	Platelet and sphere
30	Clusters	146	1.4–3	2.44	Sphere
40	Clusters	252	1.5–2.5	2.76	Sphere

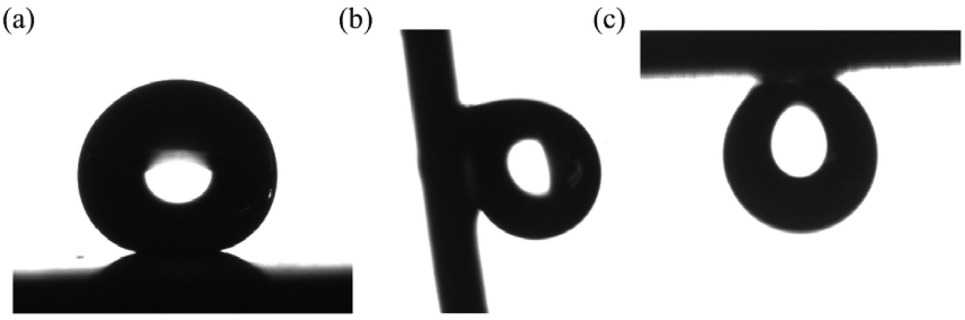

Fig. 5. Images of water droplets (3.5 μL) on the surfaces prepared with a deposition time of 20 s at different tilting angles: (a) 0°, (b) 80° and (c) 180°.

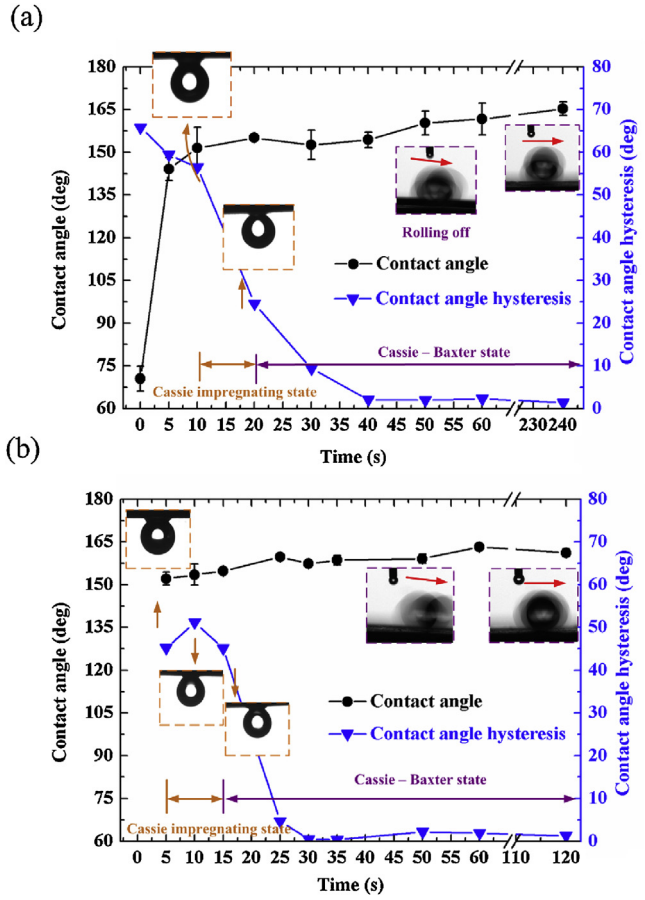

Fig. 6. CA and CAH of a water droplet on the surfaces with different deposition time. (a) Group 1 and (b) Group 2.

We also intend to investigate the correlation between the surface morphologies and wetting property. Fig. 6 provides the measured CAs and CAHs of water droplets on the silvers coated and uncoated surfaces. For the first group (Fig. 6a), it should be noticed that the uncoated copper has a CA of 70.5° and a CAH of 65.8°. So this surface is hydrophilic. While, after treatment with our proposed approach, the surfaces turn highly hydrophobic. The hydrophobicity is attributed to the sufficient roughness generated by silver deposition and the low-surface-energy surface modifier (HDFT) covering on the silver. Furthermore, when t is longer than 5 s, CAs of surfaces are found to be larger than 150° and reach to 165.3° at 240 s. According to Fig. 3, it is evident that these surfaces superhydrophobicity is given by the dual-scale hierarchical structures.

Despite the common property, Fig. 6a shows a remarkable disparity of CAHs among the hierarchically structured surfaces. The slippery wetting property was attained for the surfaces with t longer than 20 s, which exhibit CAHs less than 10°. The droplets on these surfaces easily roll off when the surfaces are tilted slightly or even laid flat. In contrast, the surfaces with t ranging from 10 to 20 s exhibit the sticky wetting property. CAH is found to be 56.5° when the surface is deposited for 10 s. In this case, 3.5 μL of water droplets can be firmly pinned on the surface without any movement when it is turned upside down (Fig. 6a). Large CAH (24.6°) is still obtained on the surface with a t of 20 s. Its sticky characteristic has been presented by Fig. 5b and c. In this study, we repeat the samples fabrication to obtain another group of surfaces. Fig. 6b presents the measurement results of CAs and CAHs for this group. The results are similar to those of the first group. When t is larger than 15 s, the surfaces exhibit the slippery superhydrophobic wetting property with CAs larger than 150° and CAHs less than 10°. While, the surface with t ranging from 5 to 15 s possess the sticky superhydrophobic property with high CAs (>150°) and large CAHs (>45°).

We use the two wetting states, Cassie-Baxter and Cassie impregnating states, to describe the wetting properties of the fabricated surfaces. A conclusion made from the measurement results (Fig. 6) is that water droplets on the surfaces with t larger than 20 s are in the Cassie-Baxter state and on the surfaces with t ranging from 5 to 20 s are in the Cassie impregnating states. It has been illustrated that the wetting states are greatly affected by surfaces structures. Table 1 has summarized the features of surfaces structures with t from 10 s to 40 s. When t is above 20 s, the microscale clusters have smaller P and larger h. It is believed that a layer of air is trapped between the surface and the droplet, resulting a three-phase solid-water-air interface. For this state, the air parts of the surface can be considered perfectly nonwetting, leading to a remarkable low water adhesion. While, the clusters of the surfaces with t no more

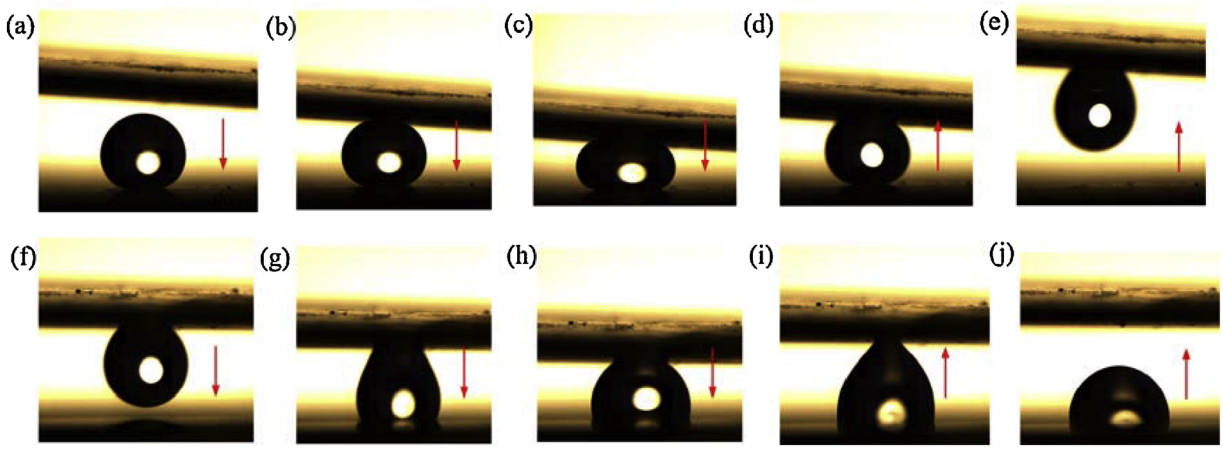

Fig. 7. Photographs showing the droplet transportation process. (a–e) Water droplets from a slippery superhydrophobic surface to a sticky superhydrophobic surface; (f–j) Water droplets from a sticky superhydrophobic surface to a hydrophilic surface.

than 20 s have lower density and height, making the droplets impregnate into the clusters. The state has an increased liquid-solid contact area, resulting in an enlarged adhesion to water. In addition, the wetting state can also be determined by the nanostructure. According to the study [12], the lower nanostructure density may lead to the droplet impregnation. For the surfaces with t no more than 20 s, the geometry of the nanostructure is platelet or combined platelet and sphere. The platelet-shaped nanostructure has the lower surface area, promoting a higher degree of impregnation.

According to the above analysis, the wetting property of the silver deposited surfaces is strongly associated with t. Taking a short t can fabricate the sticky superhydrophobic surfaces due to the formation of dual-scale hierarchical structure on which the microstructure has small density and height, and the nanostructure has low surface area.

5. Application

The prepared sticky superhydrophobic surfaces can be used as a "mechanical hand" to grasp small water droplets from a slippery superhydrophobic surface and transfer the droplets to a hydrophilic one. Since the length of shooting time is limited for the high-speed camera, we recorded the two processes separately. This first process is shown in Fig. 7a–e and Supplementary Movie 1 (see the Supplementary Material). A 3.5 μL of water droplet is first placed on the prepared slippery superhydrophobic surface with a CA of 157.4° and a CAH of 0.5°. After that, a prepared sticky superhydrophobic surface with a CA of 154.8° and a CAH of 45.1° is used to touch the droplet (Fig. 7a and b). The water droplet sticks to the surface (Fig. 7c) and departs from the slippery surface after lifting the sticky surface (Fig. 7d and e). So the droplet is successfully grasped by a sticky superhydrophobic surface. The transfer process is shown in Fig. 7f–j and Supplementary Movie 2 (see the Supplementary Material). At first, the sticky superhydrophobic surface holding a droplet moves down to touch a hydrophilic surface (Fig. 7f and g). Then, the water droplet spreads on the hydrophilic surface with the contact line increasing. After lifting the sticky superhydrophobic surface, the droplet is released on the hydrophilic surface.

6. Conclusion

In this study, a remarkably straightforward method was proposed to fabricate the sticky superhydrophobic surfaces. The fabrication used electroless galvanic deposition to coat the copper substrates with a textured layer of silver. With the precise control of deposition time, the rose petal-like hierarchical structures were achieved on the substrates. Subsequent immersion of the coated substrates in the surface modifier (HDFT) covers the textured layer with a low surface free energy monolayer and renders it hydrophobic. The prepared artificial surface shows a great sticky superhydrophobic wetting property. For example, the artificial surface with a deposition time of 10 s exhibit the superhydrophobity with a CA of 151.5°, and effective adhesion with a CAH of 56.5°. It is believed that the water droplets on this surface are on the Cassie impregnating wetting state. For this state, the droplets are impregnate between the microstructure, resulting in an enlarged adhesion to water. The prepared sticky superhydrophobic surfaces are also shown in the application of droplet transportation. In this process, this surface can act as a mechanical hand to grasp and transport the droplet.

Acknowledgments

This work was supported partly by National Science Foundation of China (51576078, 51376070), and partly by 973 Project of the Ministry of Science and Technology of China (2011CB013105). The authors would like to thank Ms. Gao Xianhui for assistance with the SEM imaging and Mr. Zhuang Shaoqin for assistance with the AFM imaging.

Appendix A. Supplementary data

Supplementary data associated with this article can be found, in the online version, at http://dx.doi.org/10.1016/j.apsusc.2016.05.128.

References

[1] W. Ming, D. Wu, R. van Benthem, G. De, With superhydrophobic films from raspberry-like particles, Nano Lett. 5 (2005) 2298–2301.
[2] Y. Li, W.P. Cai, B.Q. Cao, G.T. Duan, F.Q. Sun, C.C. Li, L.C. Jia, Two-dimensional hierarchical porous silica film and its tunable superhydrophobicity, Nanotechnology 17 (2006) 238–243.
[3] B.T. Qian, Z.Q. Shen, Fabrication of superhydrophobic surfaces by dislocation-selective chemical etching on aluminum, copper, and zinc substrates, Langmuir 21 (2005) 9007–9009.
[4] C.L. Hao, J. Li, Y. Liu, X.F. Zhou, Y.H. Liu, R. Liu, L.F. Che, W.Z. Zhou, D. Sun, L. Li, Superhydrophobic-like tunable droplet bouncing on slippery liquid interfaces, Nat. Commun. 6 (2015) 7896.
[5] T. Saison, C. Peroz, V. Chauveau, S. Berthier, E. Sondergard, H. Arribart, Replication of butterfly wing and natural lotus leaf structures by nanoimprint on silica sol–gel films, Bioinspir. Biomim. 3 (2008) 046004.

[6] M. Nosonovsky, B. Bhushan, Multiscale Dissipative Mechanisms and Hierarchical Surfaces: Friction, Superhydrophobicity, and Biomimetics, Springer-Verlag, Heidelberg, Germany, 2008.
[7] Y. Lu, S. Sathasivam, J. Song, C.R. Crick, C.J. Carmalt, I.P. Parkin, Robust self-cleaning surfaces that function when exposed to either air or oil, Science 347 (2015) 1132–1135.
[8] Y. Lu, S. Sathasivam, J. Song, W. Xu, C.J. Carmalt, I.P. Parkin, Water droplets bouncing on superhydrophobic soft porous materials, J. Mater. Chem. A 2 (2014) 12177–12184.
[9] Y. Lu, S. Sathasivam, J. Song, F. Chen, W. Xu, C.J. Carmalt, I.P. Parkin, Creating superhydrophobic mild steel surfaces for water proofing and oil–water separation, J. Mater. Chem. A 2 (2014) 11628–11634.
[10] X. Yao, Y.L. Song, L. Jiang, Applications of bio-inspired special wettable surfaces, Adv. Mater. 23 (2011) 719–734.
[11] L. Feng, Y. Zhang, J. Xi, Y. Zhu, N. Wang, F. Xia, L. Jiang, Petal effect: a superhydrophobic state with high adhesive force, Langmuir 24 (2008) 4114–4119.
[12] B. Bhushan, E.K. Her, Fabrication of superhydrophobic surfaces with high and low adhesion inspired from rose petal, Langmuir 26 (2010) 8207–8217.
[13] K.H. Cho, L.J. Chen, Fabrication of sticky and slippery superhydrophobic surfaces via spin-coating silica nanoparticles onto flat/patterned substrates, Nanotechnology 22 (2011) 445706.
[14] F. Li, Y.Y. Tu, J.W. Hu, H.L. Zou, G.J. Liu, S.D. Lin, G.H. Yang, S.Y. Hu, M. Lei, Y. Mo, Fabrication of fluorinated raspberry particles and their use as building blocks for the construction of superhydrophobic films to mimic the wettabilities from lotus leaves to rose petals, Polym. Chem. 6 (2015) 6746–6760.
[15] J. Long, P. Fan, D. Gong, D. Jiang, H. Zhang, L. Li, M. Zhong, Superhydrophobic surfaces fabricated by femtosecond laser with tunable water adhesion from lotus leaf to rose petal, ACS Appl. Mater. Interfaces 7 (2015) 9858–9865.
[16] N.D. Boscher, D. Duday, S. Verdier, P. Choquet, Single-step process for the deposition of high water contact angle and high water sliding angle surfaces by atmospheric pressure dielectric barrier discharge, ACS Appl. Mater. Interfaces 5 (2013) 1053–1060.
[17] W.S. Wong, N. Nasiri, G. Liu, N. Rumsey-Hill, V.S. Craig, D.R. Nisbet, A. Tricoli, Flexible transparent hierarchical nanomesh for rose petal-like droplet manipulation and lossless transfer, Adv. Mater. Interfaces 2 (2015) 1500071.
[18] A. Larmour, S.E.J. Bell, G.C. Saunders, Remarkably simple fabrication of superhydrophobic surfaces using electroless galvanic deposition, Angew. Chem. Int. Ed. 46 (2007) 1710–1712.
[19] J.V. Timonen, M. Latikka, O. Ikkala, R.H. Ras, Free-decay and resonant methods for investigating the fundamental limit of superhydrophobicity, Nat. Commun. 4 (2013) 2398.
[20] H. Mertaniemi, V. Jokinen, L. Sainiemi, S. Franssila, A. Marmur, O. Ikkala, R.H. Ras, Superhydrophobic tracks for low-friction, guided transport of water droplets, Adv. Mater. 23 (2011) 2911–2914.
[21] J.V. Timonen, M. Latikka, L. Leibler, R.H. Ras, O. Ikkala, Switchable static and dynamic self-assembly of magnetic droplets on superhydrophobic surfaces, Science 341 (2013) 253–257.
[22] R.N. Wenzel, Resistance of solid surfaces to wetting by water, Ind. Eng. Chem. Res. 28 (1936) 988–994.
[23] A.B.D. Cassie, S. Baxter, Wettability of porous surfaces, Trans. Faraday Soc. 40 (1944) 546–551.
[24] B. Bhushan, M. Nosonovsky, The rose petal effect and the modes of superhydrophobicity, Phil. Trans. R. Soc. A 368 (2010) 4713–4728.
[25] N.D. Boscher, V. Vaché, P. Carminati, P. Grysan, P. Choquet, A simple and scalable approach towards the preparation of superhydrophobic surfaces–importance of the surface roughness skewness, J. Mater. Chem. A 2 (2014) 5744–5750.
[26] Y.L. Zhang, H. Xia, E. Kim, H.B. Sun, Recent developments in superhydrophobic surfaces with unique structural and functional properties, Soft Matter 8 (2012) 11217–11231.
[27] F.M. Chang, S.J. Hong, Y.J. Sheng, H.K. Tsao, High contact angle hysteresis of superhydrophobic surfaces: hydrophobic defects, Appl. Phys. Lett. 95 (2009) 064102.
[28] N.J. Shirtcliffe, G. McHale, M.I. Newton, C.C. Perry, Wetting and wetting transitions on copper-based super-hydrophobic surfaces, Langmuir 21 (2005) 937–943.